Global NEST Journal, Vol 26, No 8, 05939

Electrochemically deposited zinc oxide films on stainless steel for photo degradation of Basic Red 18 dye

Doğan Cirmi[1], Zeynep Bilici[2], Nadir Dizge[2], M. Shameer Basha[3], B. Deepanraj[4]* and Jasgurpreet Singh Chohan[5]
[1]Department of Chemistry, Mersin University, Mersin, 33343, Turkey
[2]Department of Environmental Engineering, Mersin University, Mersin, 33343, Turkey
[3]Department of Mechanical Engineering, College of Engineering, Qassim University, Buraidah–51452, Saudi Arabia
[4]Department of Mechanical Engineering, Prince Mohammad Bin Fahd University, Al-Khobar, 31952, Saudi Arabia
[5]University Centre for Research & Development, Department of Mechanical Engineering, Chandigarh University, Gharuan, Punjab, India
Received: 19/03/2024, Accepted: 04/07/2024, Available online: 02/08/2024
*to whom all correspondence should be addressed: e-mail: babudeepan@gmail.com
https://doi.org/10.30955/gnj.05939

Graphical abstract

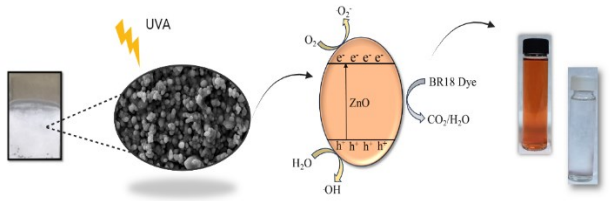

Abstract

In this study, zinc oxide (ZnO) films have been electrochemically deposited on stainless steel and its photocatalytic activity on the degradation of BR 18 dyes was tested. The effects of different electrodeposition conditions such as deposition potential and deposition time on the nanostructures of ZnO films were investigated in detail and the best electrodeposition conditions were optimized. The electrochemical, structural and morphological, were characterized by cyclic voltammetry (CV), chronoamperometry, X-ray diffraction (XRD), scanning electron microscope (SEM), respectively. The best removal efficiency was 37% at -1.2 V, and increased up to 53% after 300 sec coating. The number of electrodes (1, 2, 3 and 4 coatings) and dye concentration (5, 10, 15 mg/L) covered with -1.2 V potential and the coating synthesized in 300 seconds were studied. A complete removal was obtained when the number of electrodes covered was 4 and at 5 mg/L initial dye concentration. The number of reuses was tested up to 5 cycles. ZnO coatings on stainless steel that were electrochemically charged showed good photocatalytic stability. Because ZnO films have both economic and environmental advantages, it is imperative that they can be synthesized using environmentally benign processes and used in photocatalysis. This novel strategy provides a chance to utilize ZnO film photocatalytic characteristics for a range of environmental remediation applications in addition to providing a sustainable wastewater management solution.

Keywords: Electrodeposition, ZnO, photocatalytic oxidation, BR18 dye

1. Introduction

Water pollution is the water that is formed as a result of the use of water resources as a result of industrial, agricultural, and domestic activities and has lost its natural characteristics (Tarazona 2014, Lamkhao *et. al*. 2023). Water pollution, which is an important environmental problem throughout the world, greatly affects the lives of living things (Earnhart 2013). Wastewater from industrial activities (chemistry, metals, petroleum, leather, textiles, food, etc.) creates wastewater with a high pollution load. When these wastewaters are given to the receiving environment (rivers, lakes, seas, groundwater, etc.) without treatment, they pose serious threats to human health and disrupt the ecosystem balance (Antoniadis *et al*. 2007).Wastewater from the textile industry causes serious pollution due to the loss of 15-20% of the dyes consumed during the process (Ghalebizade and Ayati 2016). Azo dyes are common and important compounds in the textile industry that contain N=N chemical bonds. Wastewater with a high concentration of dyes originating from this industry needs to be treated because it is harmful to the environment, carcinogenic, and toxic (Roy *et al*. 2020). The textile industry frequently uses water-soluble synthetic dyes like Basic Red 18 (BR 18), which is a cationic dye (Ugur *et al*., 2021). BR 18, which is an azo dye, can destroy the aquatic environment's biological activity, produce color pollution, and reduce clarity. Moreover, synthetic azo dyes provide a significant risk to human health due to all of these factors, requiring their rapid removal from aquatic environments (Mahmoodi *et. al*. 2016).

The treatment of textile wastewater is difficult due to high flow rates and pollution (Hasanbeigi and Price 2015). Coagulation, adsorption, membrane filtration, electrocoagulation, Fenton, photo-electro Fenton and

photocatalytic systems are widely used in the treatment of textile wastewater (Tao and Wang 2023). Biological treatment is not used alone, as it is insufficient for the decomposition of dangerous aromatic compounds. Cost-intensive physical techniques include membrane filtration, coagulation, adsorption, and electrocoagulation (Naseri *et al*. 2021). Advanced oxidation processes are used to provide wastewater treatment by breaking down synthetic azo dyestuffs. These processes produce hydroxyl radicals, which degrade organic compounds and other pollutants (Naseri *et al*. 2021). Photocatalytic oxidation, one of the advanced oxidation processes, is wastewater treatment using a catalyst under sunlight or UV light (Bethi *et al*. 2016).

BR 18 dye was removed from aqueous solution using basalt powder as a heterogeneous catalyst for the Fenton and photo-Fenton reactions. The removal efficiencies for BR 18 by the Fenton and photo-Fenton process were 87% and 70%, respectively, at 70 mg/L dye concentration, 5 mM H_2O_2 concentration, 1.0 g/L basalt amount and pH 2 (Saleh *et al*. 2021). In another study, ZnO/MoS_2/rGO composite catalyst was used for photocatalytic decolorization of BR 18 dye. The results showed that 100% removal efficiency was achieved for 25ZnO/75MG2 at 25 mg/L initial dye concentration and 0.5 g/L catalyst amount for 60 min (Ugur *et al*. 2021). Eskikaya *et al*. (2022) investigated photocatalytic activity of zinc oxide nanoflowers (ZnO-NFs) for BR 18 removal from aqueous solution. ZnO-NFs were synthesized by two different processes hydrothermal method (named ZnO-NF1) and the precipitation method (named ZnO-NF2). BR 18 was completely removed at 25 mg/L BR18 dye concentration using 1.5 g/L ZnO-NF1 amount for 75 min.

Zinc oxide (ZnO) is a compound used as an important photocatalyst due to both its photocatalytic properties and its inexpensive, environmentally friendly and non-toxicity (Kohzadi *et al*. 2023). Many methods have been developed to prepare ZnO thin films such as chemical vapor deposition, sol gel, pulsed laser deposition, hydrotermal methods and electrochemical methods (Rekha *et al*. 2023). Electrochemical method has many advantages such as the mass, thickness, morphology, low-temperature processing, low cost process and good electrical contact between structures and substrate.

When ZnO is excited under sunlight, the electrons on its surface rise to higher energy levels, causing the formation of free radicals such as reactive oxygen species hydroxyl radicals (OH•) and superoxide radicals (O_2•-) (Kumar *et al*. 2021, Elshahawy *et al*. 2023). These free radicals break down organic pollutants and other harmful substances, provides them to be cleaned (Elshahawy *et al*. 2023). ZnO photocatalysis stands out as an environmentally friendly, sustainable purification and cleaning method (Selvaraj *et al*. 2022). Helping to neutralize pollutants by using a clean and renewable energy source such as sunlight contributes to reducing environmental pollution and protecting the environment (Singh, 2022). It is also used in areas such as water treatment, air cleaning, self-cleaning surfaces, energy generation (Fiorenza *et al*. 2023).

In this study, we prepared electrochemical technique of deposition ZnO film on a Stainless Steel. The effects of deposition parameters, such as the deposition time and applied potential were also investigated. It was aimed to examine the effect of ZnO on the coating under different conditions and to increase its reuse without loss of catalyst. In addition to examining the decomposition products of BR18 using a photocatalytic system, the effect of ZnO on parameters such as voltage change, H_2O_2 concentration, contact time during plating on stainless steel was studied. Kinetic, dye concentration and reuse experiments were carried out with the coating obtained under optimum conditions.

2. Material and methods

2.1. Materials

All chemicals used in this work without further purification were of analytical grade. The substrate is Stainless Steel (SS) type 316 cut with dimensions 1 cm × 2 cm. Zinc chloride **(**$ZnCl_2$, Merck, Germany), Potassium chloride **(**KCl, Merck, Germany) and Hydrogen peroxide (H_2O_2, Merck, Germany) were used. BR18 azo dyestuff was prepared as 100 mg/L stock solution in distilled water.

2.2. Electrochemical synthesis of ZnO

The electrodeposition of ZnO thin films were carried out using a potentiostat/galvanostat (CHI 660A, CH Instruments). The 316 stainless steel (SS) (1 cm × 2 cm), a Ag/AgCl (saturated KCl) and a platinum plate (1 cm × 2 cm) has been used as working electrode, reference electrode and counter electrode, respectively (Figure 1). Prior to electrodeposition, the SS substrates were ultrasound cleaned with acetone and distilled water. An aqueous solution of 0.05 M $ZnCl_2$, 0.1 M KCl and 20 mM H_2O_2 was used as electrolyte. The temperature was maintained at 70 °C throughout the deposition process. ZnO nanoparticles were distributed uniformly through electrodeposition process optimization. Investigated were the effects of electrodeposition times (120, 180, 300, and 420 sec) and potentials (from -1.1 V, -1.2 V, and -1.3 V vs. Ag/AgCl).

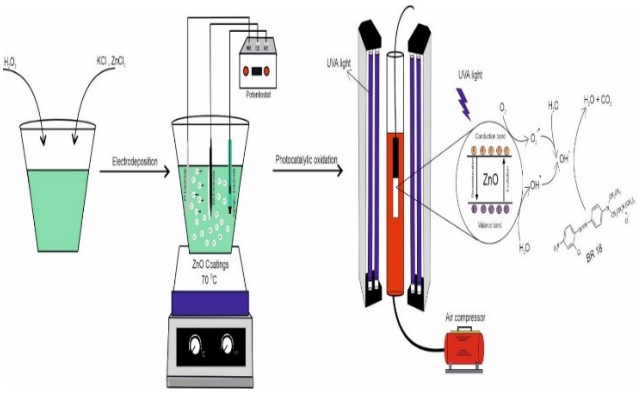

Figure 1. A schematic representation of the experimental set up

A photograph belongs to stainless steel coated with ZnO is shown in Figure. 2.

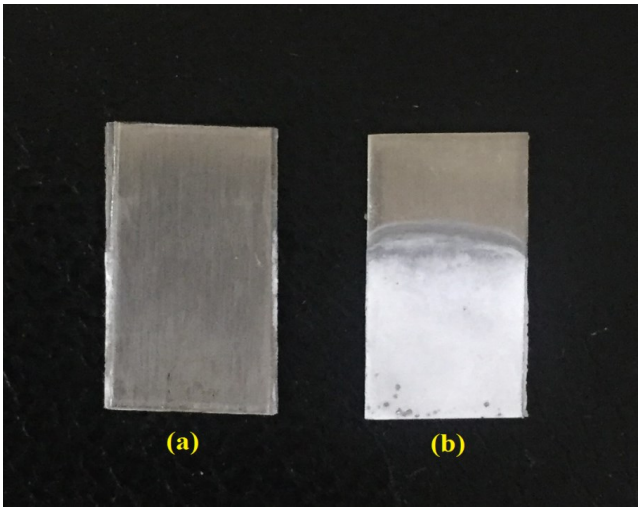

Figure 2. (a) Stainless steel, (b) ZnO-coated stainless steel

2.3. Characterization techniques

ZnO film electrodeposition was performed with a potentiostat/galvanostat (CHI 660A, CH Instruments, U.S.A.). The morphology, particle size, and elemental composition of the electrodes were examined using a scanning electron microscope (model Quanta 650) fitted with an EDX detector. The X-ray diffraction spectra (XRD) analysis was performed using Cu-Kα (λ = 1.54 Å) irradiation as an X-ray source (40 kV/30 mA) and Empyrean (PANalytical) operating in a 2θ scan from 30° to 80°.

2.4. Photocatalytic studies

In this study, ZnO coating was applied on stainless steel (1cm × 2 cm) and its photocatalytic effect on BR18 dye removal was investigated. The system was carried out using 6 UVA lamps (Philips TL8W Actinic BL) at 365 nm wavelength in a circular reactor covered with aluminum foil. The luminous intensity and wavelength of the lamps used are 3.5 mW/cm^2 and 365 nm, respectively. Firstly, 10 mg/L BR18, 10 mL volume and potential (−1.1 V, -1.2 V and -1.3 V) were studied during the 2-hour experiment. Coatings were done at different second (120,180, 300 and 420 sec) with the voltage with the best results. Then, the number of electrodes covered (1, 2, 3 and 4 coating), dye concentration (5, 10 and 15 mg/L) studies and reuse experiments were carried out. Samples taken from the reactor were measured at 484 nm wavelength using a UV-vis (T90 + UV/VIS Spectrometer, PG Instruments Ltd.) spectrophotometer. The BR18 removal efficiency was calculated using the following equation (1).

$$Removal\ Efficiency(\%) = \frac{Ci - Cf}{Ci} * 100 \quad (1)$$

where the dye concentration at initial (C_i) (mg/L) and the dye concentration at final (C_f) (mg/L) are expressed in this particular format.

3. Results and discussion

3.1. Effects of electrochemical deposition parameters on ZnO films

LSV curve for ZnO films carried out in the potential range 0 to -1.6 V vs. Ag/AgCl is shown in Figure 3.

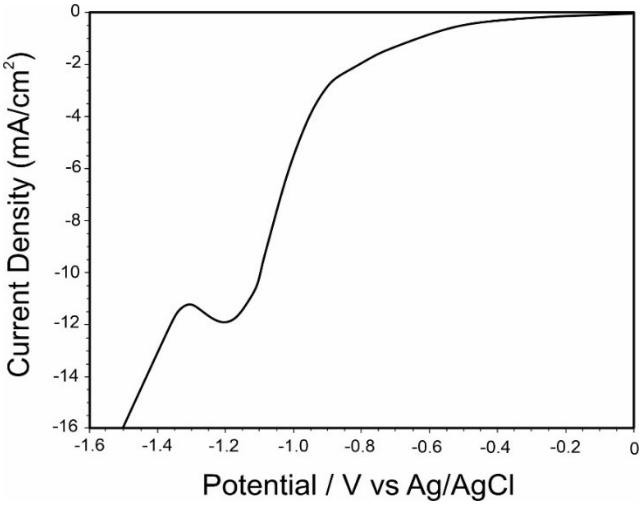

Figure 3. Linear sweep voltammetry (LSV) curves of the ZnO electrodeposition on a SS electrode from a 0.1 M KCl +20 mM H_2O_2 + 50 mM ZnCl2 solution

The ZnO film formation is based the generated OH^- by hydrogen peroxide reduction at the stainless steel interface (Pauporté and Lincot 2001).

First, the reaction that results from the reduction of hydrogen peroxide produces hydroxide ions.

$$H_2O_2 + 2e^- \rightarrow 2OH^-$$

Then, the formation of zinc hydroxide takes place by the reaction. The reaction occurs below around −1.1 V.

$$Zn^{2+} + 2(OH)^- \rightarrow Zn(OH)_2$$

The Zn $(OH)_2$ dehydrates spontaneously at higher temperature (70 °C) following:

$$Zn(OH)_2 \rightarrow ZnO + H_2O$$

Figure 4a despicts the current density curves after the application of an applied potential from –1.1 to –1.3 V at a constant temperature (70°C). In order to avoid the formation of H_2 at potentials more negative than -1.3 V, coating processes were not carried out. As expected, it was observed that high current density occurs with the increase of applied cathodic potentials. The cathodic current is directly related to the nucleation rate. As the cathodic current increases, the nucleation steps occur faster. Increasing the nucleation rate supports the presence of high amounts of Zn(II) ions around the electrode (Patella *et al*. 2022). This allows ZnO particles to grow vertically on the electrode surface. Figure 4b–d shows the SEM images of ZnO films deposited at potential −1.1V, −1.2V, and −1.3V, respectively. It can be seen that the type of ZnO seed layers is in the form of nanospheres. Every film exhibits compact and homogeneous deposition. ZnO nanospheres that were deposited at -1.2 V had a mixed morphology, with uniform grains arranged in irregularly shaped clusters and no homogeneous distributions, in contrast to compact, homogeneous, and uniform ZnO nanospheres. For these reasons, the applied potential was determined as -1.2 V to create a good synergistic effect between the density of the ZnO nanospheres and the active surface area.

Figure 5a shows LSV curves of different ZnO growths on SS surface as a function of the electrodeposition time. Figure 5b and 5c shows the SEM images of ZnO films deposited at time 120 and 420 s, respectively. It can be observed that two ZnO films appeared of sphere shape grown perpendicularly on a SS substrate. The SEM images show that amount of ZnO nanospheres and clustering strongly increases with increasing deposition time. ZnO nanospheres covered the entire stainless steel surface due to the increased deposition time from 120, 180, 300 and 420 sec.

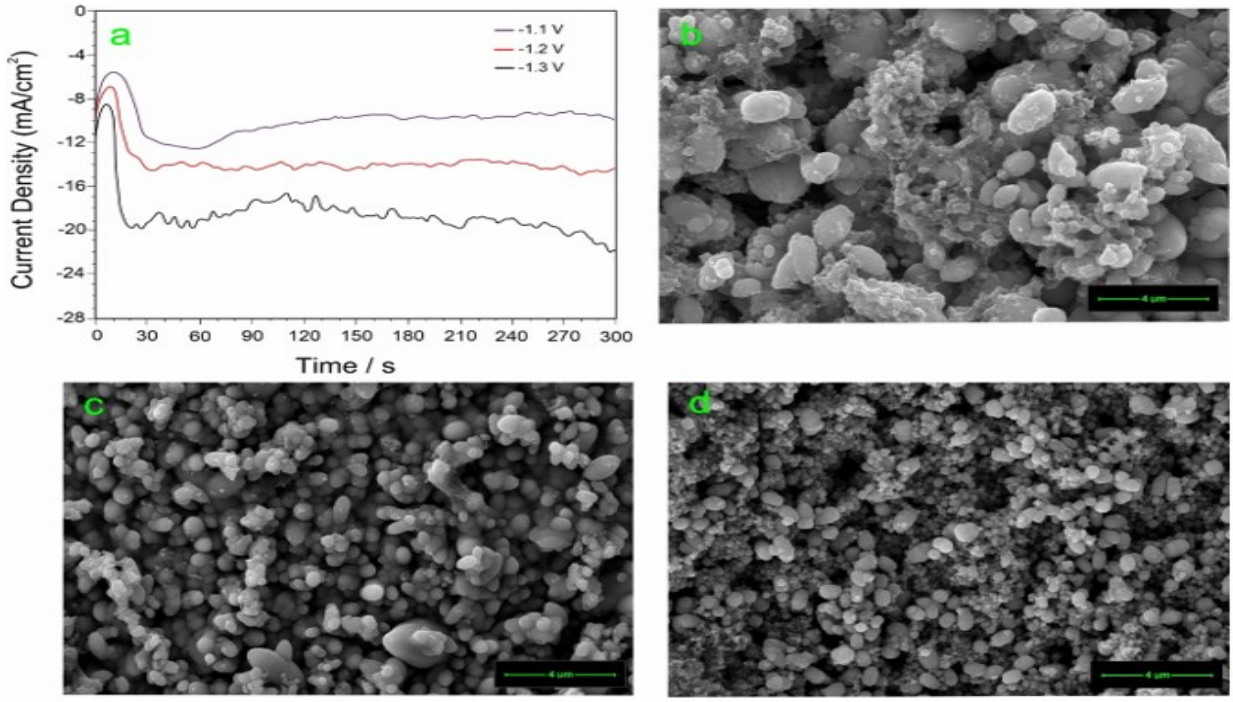

Figure 4. (a) Chronoamperometric curves and SEM images, (b) -1.1 V, (c) -1.2 V and (d)-1.3 V vs. Ag/AgCl of the ZnO electrodeposition on a SS electrode for 300 s

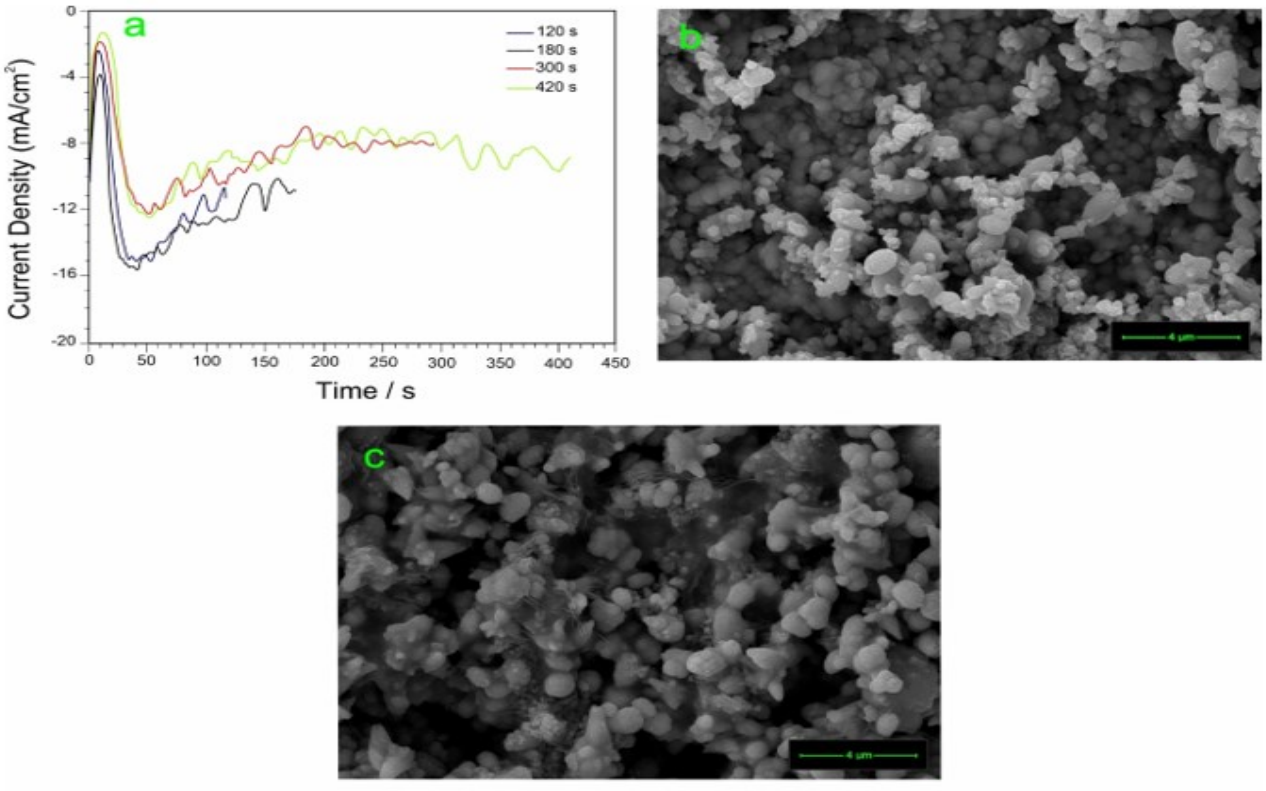

Figure 5. (a) Chronoamperometric curves and SEM images, (b) 120 sec, and (c) 420 sec of the ZnO electrodeposition on a SS electrode at -1.2 V vs. Ag/AgCl

The XRD pattern results of ZnO film is showed in Figure 6. All the diffraction peaks correspond to the ZnO wurtzite structure. The diffraction peaks at 2θ = 31.74°, 34.38°, 36.21°, 47.48°, 56.55°, 62.81°, 64.79° and 68.05° corresponding to the diffraction planes of (100), (002), (101), (102), (110), (103), (200) and (112), respectively. This matches the standard values JPDS card no: 00-36-1451. The Debye-Scherrer formula was used to determine the diameter of the synthesized ZnO nanoparticle (Shirvani and Naji 2023):

$$d = \frac{K\lambda}{\beta \cos \theta} \quad (6)$$

In this case, K is a constant of 0.9, β is the full width at half maximum (FWHM) in radians, λ is the Bragg angle, and λ is the wavelength of the X-ray (1.5406 Å). A ZnO crystallite size average of 17.70 nm was determined.

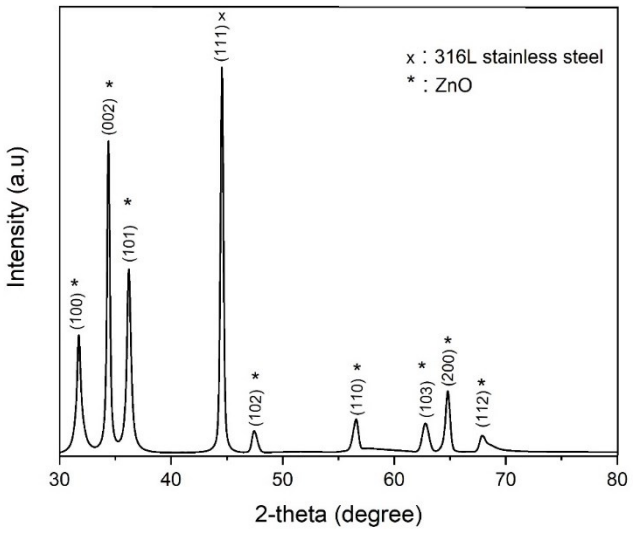

Figure 6. X-ray diffractograms of ZnO films electrodeposited at -1.2 V vs. Ag/AgCl

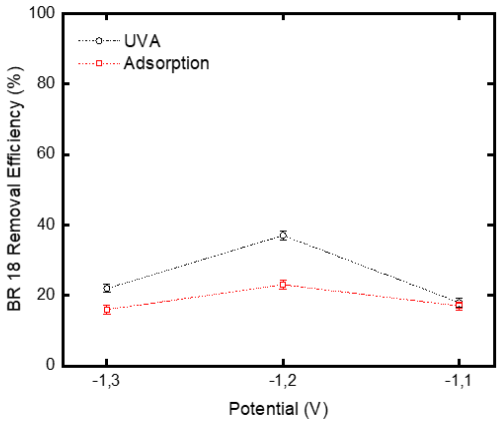

Figure 7. Effect of different potentials on dye removal efficiency

3.2. Effect of BR18 removal efficiency at different potentials

Coatings carried out at different potentials from -1.1 to -1.3 V for 180 sec were investigated on the effect of BR18 dye removal efficiency. Both photocatalytic oxidation and adsorption studies were carried out under the same conditions. The study was carried out with 10 mg/L BR18 dye concentration, 2 hours of experimentation and 1 coating (1 cm × 2 cm). The BR18 removal efficiency graph is given in Figure 7. The coatings made at -1.1 V, -1.2 V and -1.3 V potentials obtained 18%, 37% and 22% removal efficiency under UVA light, respectively. In the adsorption study, 17%, 23% and 16% removal efficiencies were achieved.

3.3. The effect of surfaces coated at different times

According to the potential values, the best dye removal efficiency was realized at -1.2 V. For this reason, further studies were continued with coatings produced at -1.2 V. After the coatings were made at 120, 180, 300 and 420 seconds, BR18 removal efficiency in UVA and adsorption was checked for 10 mg/L BR18 dye concentration. The dye removal efficiency graph depending on the coating time is given in Figure 8. In the photocatalytic study, 28%, 37%, 53% and 32% removal efficiencies were obtained at 120, 180, 300 and 420 sec, respectively; 18%, 23%, 19% and 16% removal efficiencies were obtained in the adsorption study. Therefore, 300 sec coating was chosen for further experiments due to obtaining the highest removal efficiency.

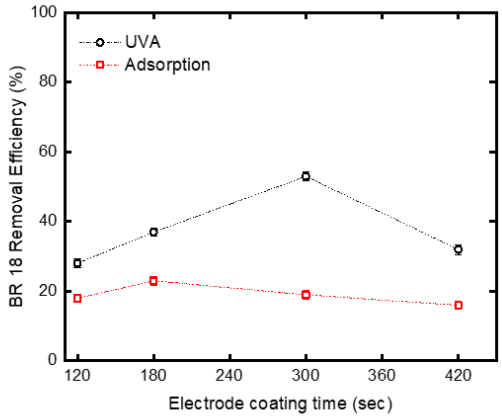

Figure 8. Effect of different ZnO coating times on dye removal efficiency

3.4. Effect of coating numbers on dye removal efficiency

The study was continued with the best conditions obtained at -1.2 V and 300 sec coating. The time dependent dye removal efficiency graph according to the number of coatings is shown in Figure 9. While 53.0% removal efficiency was obtained for 1 coating, 59.9% removal efficiency was obtained for 2 coatings, 73.6% for 3 coatings and 80.2% for 4 coatings for 10 mg/L BR18 dye concentration.

In the study conducted by Xu *et al*. 2020, a sol-gel method was used to deposit Al-doped ZnO coatings on stainless steel wire mesh. It was observed that the removal efficiency increased as the amount of ZnO photocatalyst loaded on the stainless steel wire mesh increased. It is proportional to the higher photocatalytic activity that the ZnO catalyst is covered with more surface area (Xu *et al*. 2020).

In another study, ZnO aggregations were developed on compacted stainless steel cages and their photocatalytic effect was examined. It exhibited an improved photocatalytic property performance compared to the degradation of RhB under UVA light. In the photocatalysis degradation reaction, when the hierarchical aggregation had larger surface area, it offered more reaction area due to the larger porous channels in the nanolayers (Li *et al*. 2016).

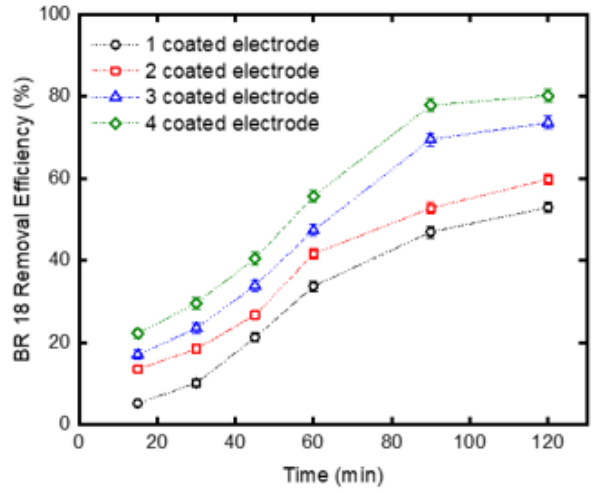

Figure 9. The effect of the number of coatings on the dye removal efficiency

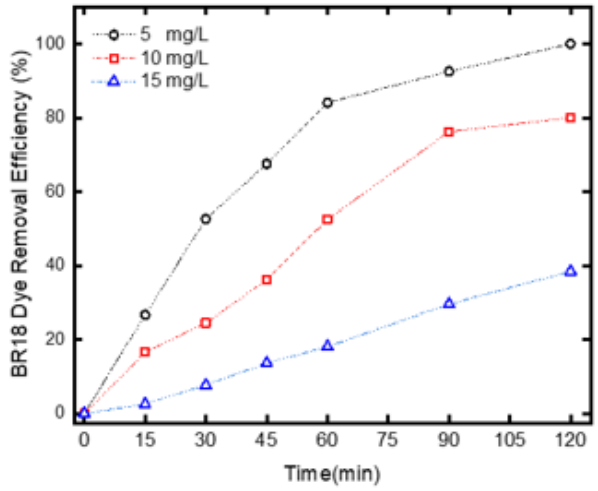

Figure 10. Effect of dye concentration on time-dependent removal efficiency

3.5. Effect of dye concentration

According to previous experiments, optimum conditions were determined as -1.2 V potential, 300 sec coating time and 4 coatings. In these conditions, the time-dependent dye removal efficiency of 5, 10 and 15 mg/L was investigated. At 5 mg/L, 26% at 15 min and 100% at 120 min were obtained. While it reached from 16% to 80% at 10 mg/L, removal efficiency from 2% to 38% was reached at 15 mg/L. Effect of dye concentration on time-dependent removal efficiency is given in Figure 10. This decrease is attributed to the decrease in light absorption on the catalyst surface with increasing dye concentration. In addition, photo-elimination is associated with insufficient OH· radical formation. Shubha *et al*. 2023 investigated the photocatalytic degradation of textile dyes with nickel oxide (NiO-SD) NPs. Malachite green (MG) and methylene blue (MB) were used in the study. The dye concentration was tested for 4.8, 12 and 16 mg/L. It was observed that the removal efficiency of both dyes decreased significantly as the dye concentration increased (Shubha *et al*. 2023).

3.6. Reuse cycle

The reuse of the synthesized material under optimum conditions was studied. In previous studies, optimum conditions were determined as 5 mg/L BR18 concentration, 4 coatings, 300 sec coating time and -1.2 V potential. After the coating was washed with distilled water after each use, dye was added and reuse studies were continued. The reuse graph is given in Figure 11. While 100% removal efficiency was obtained in the 1st and 2nd reuses, 95% removal efficiency were obtained after 5th subsequent uses. Xu *et al*. 2020 was used for photocatalytic degradation of MB several times under the same operating conditions. After four times of photocatalytic reaction, it was observed that the degradation efficiency of the catalyst was not greatly reduced, thus the catalyst exhibited a good condition in terms of reusability. The slight decrease in the photocatalytic activity of the catalyst is explained as the changes in the surface modification due to the photocorrosion of ZnO (Xu *et al*. 2020).

In another study, photodegradation of RhB was observed over ten cycles. After each cycle, the catalyst was washed several times using deionized water and fresh RhB solution was added. The constant photodegradation rate over ten consecutive cycles showed that the catalyst was stable under different light intensity (Li *et al*. 2016).

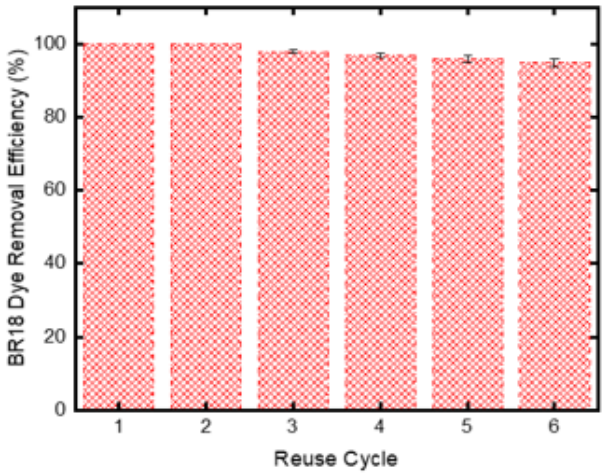

Figure 11. Reuse cycle of BR 18 dye photo-degradation

The proposed photo degradation mechanism of BR 18 dye using electrochemically deposited zinc oxide films on stainless steel are illustrated in Scheme 1.

4. Conclusion

In this study, ZnO films were successfully deposited onto on a stainless steel by electrochemical method. The effect of ZnO films on dye removal by photocatalytic oxidation was investigated. Deposition parameters such as deposition time and deposition potential in electroplating are optimized for the preparation of ZnO films with the largest

surface area, particle distribution and good catalytic effect for dye removal efficiency.

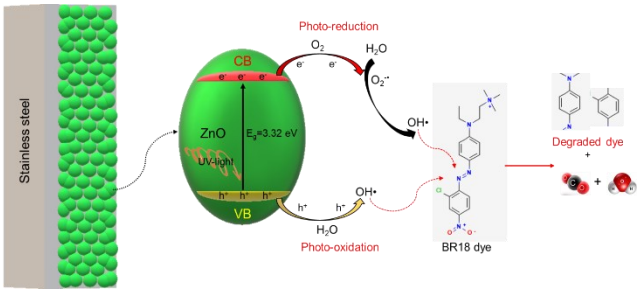

Scheme 1. Schematic illustrations for photocatalytic degradation mechanism of BR18 dye

Potentially the best dye removal efficiency was also obtained, while the best removal efficiency was obtained at 300 sec in time. The BR18 removal efficiency was achieved by performing the number of electrodes covered (1, 2, 3 and 4 coating) and dye concentration (5, 10 and 15 mg/L) tests with the coating obtained at the best potential and time. For 10 mg/L BR18 concentration, 53% removal efficiency was obtained for 1 coating, while it increased to 80.2% for 4 coatings. In dye concentration, 100%, 80% and 38.5% removal efficiency was obtained at 5, 10 and 15 mg/L, respectively, by using 4 electrode coatings. With -1.2 V potential, 300 sec coating time, 4 coated electrodes and 5 mg/L dye concentration, 100% removal efficiency was achieved and reuse studies were carried out under these conditions. It was reused 5 times and 100% removal efficiency was achieved in the first 2 uses. In subsequent use, removal efficiency decreased to 95% after 5th repeated use.

References

Antoniadis A., Takavakoglou V., Zalidis G. and Poulios I. (2007). Development and evaluation of an alternative method for municipal wastewater treatment using homogeneous photocatalysis and constructed wetlands. *Catalysis Today*, **124**(3): 260–265.

Bethi B., Sonawane S.H. Bhanvase B.A. and Gumfekar S.P. (2016). Nanomaterials-based advanced oxidation processes for wastewater treatment: A review. *Chemical Engineering and Processing–Process Intensification* **109**: 178–189.

Earnhart D. (2013). Water Pollution from Industrial Sources. Encyclopedia of Energy, Natural Resource, and Environmental Economics. *J. F. Shogren. Waltham, Elsevier***:** 114–120.

Elshahawy M.F., Abd A.N., Mohamed, R.D., El-Hag A.A. (2023). Radiation synthesis and photocatalytic performance of floated graphene oxide decorated ZnO/ alginate-based beads for methylene blue degradation under visible light irradiation. *International Journal of Biological Macromolecules* **243,** 125121.

Eskikaya O., Ozdemir S., Tollu G., Dizge N., Ramaraj R., Manivannan A. and Balakrishnan D. (2022). Synthesis of two different zinc oxide nanoflowers and comparison of antioxidant and photocatalytic activity. *Chemosphere*, **306**: 135389.

Fiorenza R., Spitaleri L., Perricelli F., Nicotra G., Fragalà M.E., Scirè S. and Gulino A. (2023). Efficient photocatalytic oxidation of VOCs using ZnO@Au nanoparticles. *Journal of Photochemistry and Photobiology A: Chemistry* **434**: 114232.

Ghalebizade M. and Ayati B. (2016). Solar photoelectrocatalytic degradation of Acid Orange 7 with ZnO/TiO2 nanocomposite coated on stainless steel electrode. *Process Safety and Environmental Protection* **103**: 192–202.

Hasanbeigi A. and Price L. (2015). A technical review of emerging technologies for energy and water efficiency and pollution reduction in the textile industry. *Journal of Cleaner Production* **95**: 30–44.

Kohzadi S., Maleki A., Bundschuh M., Vahabzadeh Z., Johari S.A., Rezaee R., Shahmoradi B., Marzban N. and Amini N. (2023). Doping zinc oxide (ZnO) nanoparticles with molybdenum boosts photocatalytic degradation of Rhodamine b (RhB): Particle characterization, degradation kinetics and aquatic toxicity testing. *Journal of Molecular Liquids* **385**: 122412.

Kumar S., Kaushik R.D. and Purohite L.P. (2021). Novel ZnO tetrapod-reduced graphene oxide nanocomposites for enhanced photocatalytic degradation of phenolic compounds and MB dye. *Journal of Molecular Liquids* **327**, 114814.

Lamkhao S., Tandorn S., Rujijanagul G., Randorn, C. (2023). A practical approach using a novel porous photocatalyst/hydrogel composite for wastewater treatment. *Materials Today Sustainability*, 100482.

Li Z., Liu G., Zhang Y., Zhou Y., Yang Y. (2016). Porous nanosheet-based hierarchical zinc oxide aggregations grown on compacted stainless steel meshes: Enhanced flexible dye-sensitized solar cells and photocatalytic activity. *Materials Research Bulletin* **80**, 191–199.

Rekha S.M., Neelamana H.V., Bhat S.V. (2023). Recent Advances in Solution-Processed Zinc Oxide Thin Films for Ultraviolet Photodetectors. *ACS Applied Electronic Materials* **5**(8), 4051–4066.

Mahmoodi N.M., Hosseinabadi-Farahani Z., Chamani H. (2016). Synthesis of nanostructured adsorbent and dye adsorption modeling by an intelligent model for multicomponent systems. *Korean Journal of Chemical and Engineering*., **33**(3), 902–913.

Naseri A., Samadi M., Pourjavadi A., Ramakrishna S. and Moshfegh A.Z. (2021). Enhanced photocatalytic activity of ZnO/g-C3N4 nanofibers constituting carbonaceous species under simulated sunlight for organic dye removal. *Ceramics International* **47**(18): 26185–26196.

Patella B., Moukri N., Regalbuto G., Cipollina C., Pace E., Di Vincenzo S., Aiello G., O'Riordan A. and Inguanta R. (2022). Electrochemical Synthesis of Zinc Oxide Nanostructures on Flexible Substrate and Application as an Electrochemical Immunoglobulin-G Immunosensor. *Materials* **15**(3): 713.

Pauporté T. and Lincot D. (2001). Hydrogen peroxide oxygen precursor for zinc oxide electrodeposition II—Mechanistic aspects. *Journal of Electroanalytical Chemistry* **517**(1): 54–62.

Roy M., Sen P. and Pal P. (2020). An integrated green management model to improve environmental performance of textile industry towards sustainability. *Journal of Cleaner Production* **271**: 122656.

Saleh M., Bilici Z., Kaya M., Yalvac M., Arslan H., Yatmaz H.C. and Dizge N. (2021). The use of basalt powder as a natural heterogeneous catalyst in the Fenton and Photo-Fenton oxidation of cationic dyes. *Advanced Powder Technology*, **32**(4): 1264–1275.

Selvaraj S., Patrick S.D, Vangari G.A. Mohan M.K., Ponnusamy S. and Muthamizchelvan C. (2022). Facile synthesis of Sm doped ZnO nanoflowers by Co-precipitation method for enhanced

photocatalytic degradation of MB dye under sunlight irradiation. *Ceramics International* **48**(19, Part B): 29049–29058.

Shirvani M. and Naji L. (2023). Comparative study on the electrochemical synthesis of zinc oxide nanorods using chronoamperometry and chronopotentiometry and their application in inverted polymer solar cells. Colloids and Surfaces A: *Physicochemical and Engineering Aspects* **660**: 130889.

Shubha J.P., Savitha H.S., Patil R.C., Assal M.E., Shaik M.R., Kuniyil M., Alduhaish O., Dubasi N. and Adil S.F. (2023). A green approach for the degradation of toxic textile dyes by nickel oxide (NiO-SD) NPs: Photocatalytic and kinetic approach. *Journal of King Saud University–Science* **35**(7): 102784.

Singh S. (2022). Natural sunlight driven photocatalytic performance of Ag/ZnO nanocrystals. *Materials Today Communications* **33**, 104438.

Tao P. and Wang Y. (2023). Enhanced photocatalytic performance of W-doped TiO2 nanoparticles for treatment of Procion Red MX-5B azo dye in textile wastewater. *International Journal of Electrochemical Science* **18**(9): 100261.

Tarazona J.V. (2014). Pollution, Water. Encyclopedia of Toxicology (Third Edition). P. Wexler. Oxford, Academic Press**:** 1024-1027.

Ugur N. Bilici Z. Ocakoglu K. Dizge N. (2021). Synthesis and characterization of composite catalysts comprised of ZnO/MoS2/rGO for photocatalytic decolorization of BR 18 dye. *Colloids and Surfaces A: Physicochemical and Engineering Aspects*, **626**: 126945.

Xu L., Xian F., Pei S., Zhu Y. (2020). Photocatalytic degradation of organic dyes using ZnO nanorods supported by stainless steel wire mesh deposited by one-step method. *Optik* **203**: 164036.